

# Supplementary Information

## Impact of Electrode Density of States on Transport through Pyridine-Linked Single Molecule Junctions

Olgun Adak<sup>1</sup>, Richard Korytár<sup>2</sup>, Andrew Y. Joe<sup>1</sup>,  
Ferdinand Evers<sup>3</sup>, and Latha Venkataraman<sup>4</sup>

<sup>1</sup>Department of Applied Physics and Applied Mathematics, Columbia University, New York, NY 10027, United States

<sup>2</sup>Institute of Nanotechnology, Karlsruhe Institute of Technology, 76344 Karlsruhe, Germany

<sup>3</sup>Institute of Theoretical Physics, University of Regensburg, D-93040 Regensburg, Germany

<sup>4</sup>Department of Applied Physics and Applied Mathematics, and Department of Chemistry, Columbia University, New York, NY 10027, United States

AUTHOR EMAIL ADDRESS: lv2117@ columbia.edu,  
ferdinand.evers@physik.uni-regensburg.de

## Contents

<b>1</b>	<b>Experimental Setup and Measurement Details</b>	<b>2</b>
<b>2</b>	<b>Two-dimensional Conductance versus Displacement Histograms</b>	<b>2</b>
<b>3</b>	<b>Derivation of Model Equations</b>	<b>3</b>
<b>4</b>	<b>Finite Temperature Effects</b>	<b>6</b>
<b>5</b>	<b>The Impact of Bias Voltage on Level Alignment and Coupling in Au Junctions</b>	<b>6</b>
<b>6</b>	<b>The Comparison Between Experimental and Simulated IV's</b>	<b>7</b>
<b>7</b>	<b>The Impact of Asymmetric Coupling on the Experimental Technique</b>	<b>8</b>
<b>8</b>	<b>Relativistic and non-Relativistic DFT Calculations</b>	<b>11</b>
<b>9</b>	<b>References</b>	<b>11</b>

# 1 Experimental Setup and Measurement Details

The block diagram of the experimental setup is shown in SI Figure S1A. A voltage is applied to the junction using a digital to analog converter (NI PXI-4461), while the current through the junction is converted to voltage using a transimpedance amplifier (Femto DLPCA-200) with bandwidth 200 kHz. The voltage output of the transimpedance amplifier is recorded at 100 kHz using A/D inputs on the NI PXI-4461.

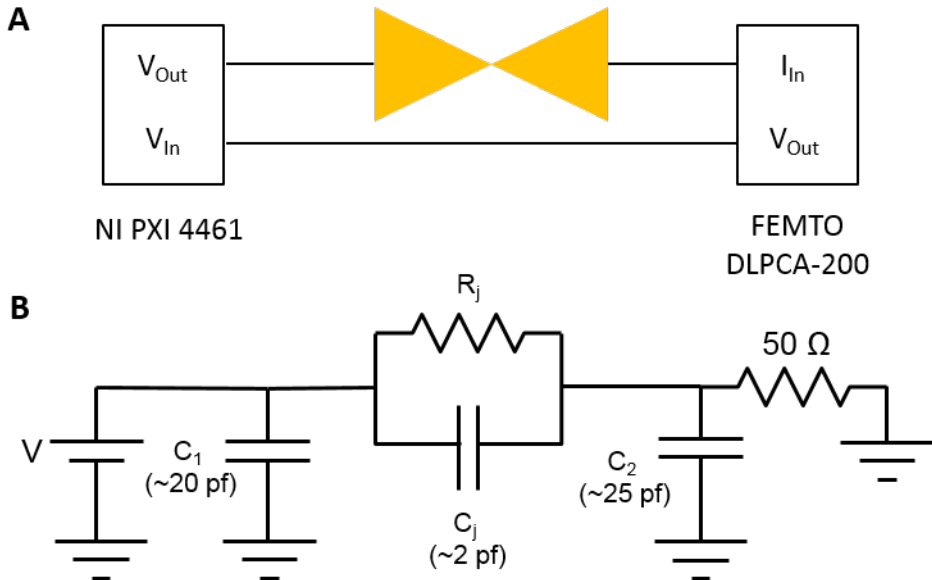


Figure S1. (A) Block diagram of STM-BJ set-up. (B) Details of the circuit showing all resistances and capacitances..

SI Figure S1B shows the circuit diagram:  $C_1$ ,  $C_2$  are the cable capacitances,  $C_j$  denotes the junction capacitance. The transimpedance amplifier has a  $50 \Omega$  input impedance. Since any current that passes through  $C_1$  does not go through the junction,  $C_1$  does not affect the measured current.  $C_2$  is in parallel with the transimpedance amplifier. At 50 kHz, the impedance of  $C_2$  is  $1.3 \times 10^5 \Omega$  is not comparable to  $50 \Omega$  input impedance of the amplifier thus  $C_2$  does not affect the measurement.  $C_j$  gives rise to capacitive currents. Therefore, the tunneling current is extracted by considering only the component of the measured current that is in-phase with the applied voltage.

## 2 Two-dimensional Conductance versus Displacement Histograms

In SI Figure S2, we show two-dimensional conductance versus displacement histograms for all the molecular systems studied. We observe a clear molecular feature indicative of junction

formation and rupture. We note that the molecular feature extends to longer lengths with Ag electrodes when compared to Au electrodes, as has been observed and explained previously.<sup>1</sup>

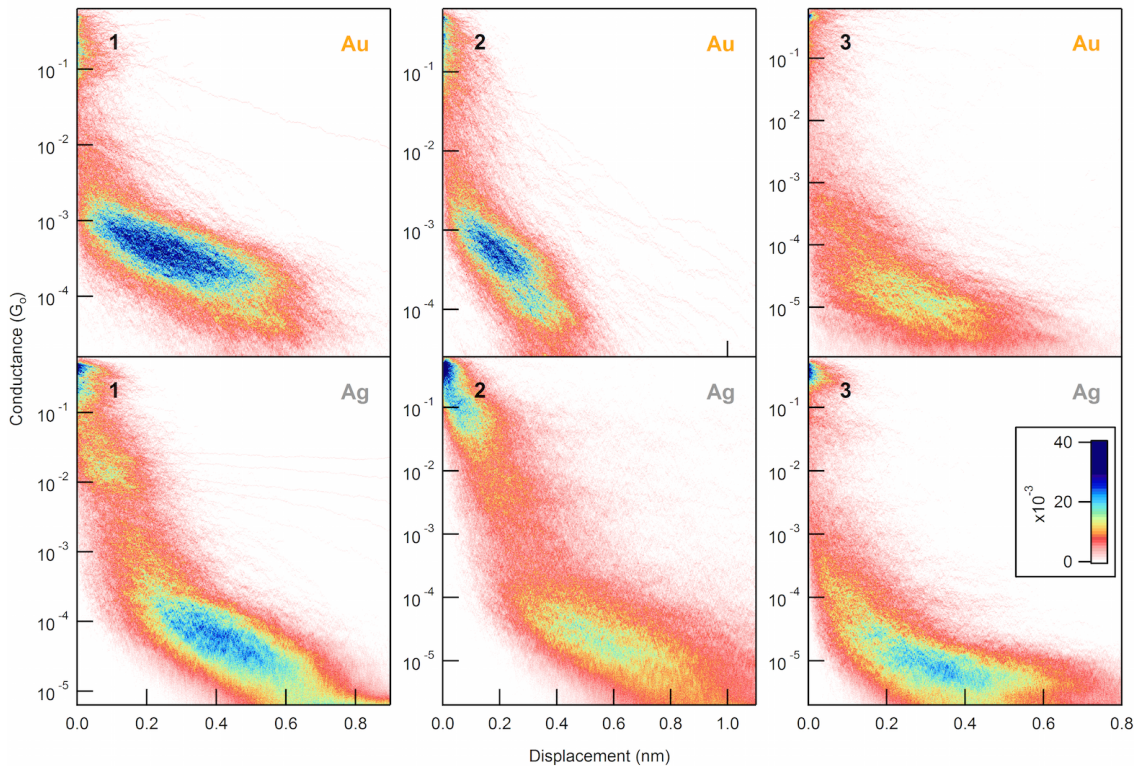


Figure S2. Normalized two-dimensional conductance-displacement histograms for measurements with Au (upper panel) and Ag (lower panel) electrodes using molecules (A) **1**, (B) **2** and (C) **3**.

### 3 Derivation of Model Equations

Taylor expansion of  $I(V)$  at  $V_o$  is given as

$$\begin{aligned}
 I(V) = & I(V_o) + \left. \frac{dI}{dV} \right|_{V=V_o} (V - V_o) + \frac{1}{2} \left. \frac{d^2I}{dV^2} \right|_{V=V_o} (V - V_o)^2 \\
 & + \frac{1}{6} \left. \frac{d^3I}{dV^3} \right|_{V=V_o} (V - V_o)^3 + \frac{1}{24} \left. \frac{d^4I}{dV^4} \right|_{V=V_o} (V - V_o)^4 \\
 & + \frac{1}{120} \left. \frac{d^5I}{dV^5} \right|_{V=V_o} (V - V_o)^5 + \frac{1}{720} \left. \frac{d^6I}{dV^6} \right|_{V=V_o} (V - V_o)^6 + \dots
 \end{aligned} \tag{1}$$

Using  $V = V_{DC} + V_{AC} \text{Sin } \omega_{AC}t$  and  $V_o = V_{DC}$ , we obtain

$$\begin{aligned}
I(t) = & I(V_{DC}) + \left. \frac{dI}{dV} \right|_{V=V_{DC}} V_{AC} \text{Sin } \omega_{AC} t + \frac{1}{2} \left. \frac{d^2 I}{dV^2} \right|_{V=V_{DC}} (V_{AC} \text{Sin } \omega_{AC} t)^2 \\
& + \frac{1}{6} \left. \frac{d^3 I}{dV^3} \right|_{V_0} (V_{AC} \text{Sin } \omega_{AC} t)^3 + \frac{1}{24} \left. \frac{d^4 I}{dV^4} \right|_{V=V_{DC}} (V_{AC} \text{Sin } \omega_{AC} t)^4 \\
& + \frac{1}{120} \left. \frac{d^5 I}{dV^5} \right|_{V=V_{DC}} (V_{AC} \text{Sin } \omega_{AC} t)^5 + \frac{1}{720} \left. \frac{d^6 I}{dV^6} \right|_{V=V_{DC}} (V_{AC} \text{Sin } \omega_{AC} t)^6 + \dots
\end{aligned} \tag{2}$$

where  $V_{DC}$  is the DC voltage,  $V_{AC}$  is the AC voltage with angular frequency  $\omega_{AC}$ . Using Fourier series expansion including terms up to the sixth order, we find

$$\begin{aligned}
I(t) = & I(V_{DC}) + \left. \frac{V_{AC}^2}{4} \frac{d^2 I}{dV^2} \right|_{V=V_{DC}} + \left. \frac{V_{AC}^4}{64} \frac{d^4 I}{dV^4} \right|_{V=V_{DC}} + \left. \frac{V_{AC}^6}{2304} \frac{d^6 I}{dV^6} \right|_{V=V_{DC}} \\
& + \text{Sin}(\omega_{AC} t) \left( \left. \frac{dI}{dV} \right|_{V=V_{DC}} V_{AC} + \left. \frac{V_{AC}^3}{8} \frac{d^3 I}{dV^3} \right|_{V_0} + \left. \frac{V_{AC}^5}{192} \frac{d^5 I}{dV^5} \right|_{V=V_{DC}} \right) \\
& - \text{Cos}(2\omega_{AC} t) \left( \left. \frac{V_{AC}^2}{4} \frac{d^2 I}{dV^2} \right|_{V=V_{DC}} + \left. \frac{V_{AC}^4}{48} \frac{d^4 I}{dV^4} \right|_{V=V_{DC}} + \left. \frac{V_{AC}^6}{1536} \frac{d^6 I}{dV^6} \right|_{V=V_{DC}} \right) \\
& - \text{Sin}(3\omega_{AC} t) \left( \left. \frac{V_{AC}^3}{24} \frac{d^3 I}{dV^3} \right|_{V_0} + \left. \frac{V_{AC}^5}{384} \frac{d^5 I}{dV^5} \right|_{V=V_{DC}} \right) \\
& + \text{Cos}(4\omega_{AC} t) \left( \left. \frac{V_{AC}^4}{192} \frac{d^4 I}{dV^4} \right|_{V=V_{DC}} + \left. \frac{V_{AC}^6}{3840} \frac{d^6 I}{dV^6} \right|_{V=V_{DC}} \right) \\
& + \text{Sin}(5\omega_{AC} t) \left. \frac{V_{AC}^5}{1920} \frac{d^5 I}{dV^5} \right|_{V=V_{DC}} \\
& - \text{Cos}(6\omega_{AC} t) \left. \frac{V_{AC}^6}{23040} \frac{d^6 I}{dV^6} \right|_{V=V_{DC}}
\end{aligned} \tag{3}$$

When the transmission function takes a Lorentzian form, and when the applied bias voltage drops symmetrically across the junction, the relation between current and voltage in the zero-temperature limit becomes

$$I(V) = \frac{G_0}{e} \int_{-eV/2}^{eV/2} \frac{\Gamma^2/4}{(E - E_{level})^2 + \Gamma^2/4} dE \tag{4}$$

where  $E_{level}$  is the energy difference between the frontier molecular orbital and the metal Fermi level,  $\Gamma$  is the molecular orbital coupling strength,  $V$  is the bias voltage,  $G_0 = 2e^2/h$  is the conductance quantum. Upon integration, one obtains:

$$I = \frac{1}{2e}G_0\Gamma \tan^{-1}\left(\frac{eV - 2E_{level}}{\Gamma}\right) + \frac{1}{2e}G_0\Gamma \tan^{-1}\left(\frac{eV + 2E_{level}}{\Gamma}\right) \quad (5)$$

The first six derivative of  $I(V)$  with respect to  $V$  are:

$$\frac{dI}{dV} = \frac{G_0}{2e} \frac{1}{\left(\frac{4\left(\frac{eV}{2} - E_{level}\right)^2}{\Gamma^2} + 1\right)} + \frac{G_0}{2e} \frac{1}{\left(\frac{4\left(\frac{eV}{2} + E_{level}\right)^2}{\Gamma^2} + 1\right)} \quad (6)$$

$$\frac{d^2I}{dV^2} = -\frac{2G_0}{e\Gamma^2} \frac{\left(\frac{eV}{2} + E_{level}\right)}{\left(\frac{4\left(\frac{eV}{2} + E_{level}\right)^2}{\Gamma^2} + 1\right)^2} - \frac{2G_0}{e\Gamma^2} \frac{\left(\frac{eV}{2} - E_{level}\right)}{\left(\frac{4\left(\frac{eV}{2} - E_{level}\right)^2}{\Gamma^2} + 1\right)^2} \quad (7)$$

$$\begin{aligned} \frac{d^3I}{dV^3} = & -\frac{G_0}{e\Gamma^2 \left(\frac{4\left(\frac{eV}{2} + E_{level}\right)^2}{\Gamma^2} + 1\right)^2} - \frac{G_0}{e\Gamma^2 \left(\frac{4\left(\frac{eV}{2} - E_{level}\right)^2}{\Gamma^2} + 1\right)^2} \\ & + \frac{16G_0 \left(\frac{eV}{2} - E_{level}\right)^2}{e\Gamma^4 \left(\frac{4\left(\frac{eV}{2} - E_{level}\right)^2}{\Gamma^2} + 1\right)^3} + \frac{16G_0 \left(\frac{eV}{2} + E_{level}\right)^2}{e\Gamma^4 \left(\frac{4\left(\frac{eV}{2} + E_{level}\right)^2}{\Gamma^2} + 1\right)^3} \end{aligned} \quad (8)$$

$$\begin{aligned} \frac{d^4I}{dV^4} = & -\frac{192G_0 \left(\frac{eV}{2} - E_{level}\right)^3}{e\Gamma^6 \left(\frac{4\left(\frac{eV}{2} - E_{level}\right)^2}{\Gamma^2} + 1\right)^4} - \frac{192G_0 \left(\frac{eV}{2} + E_{level}\right)^3}{e\Gamma^6 \left(\frac{4\left(\frac{eV}{2} + E_{level}\right)^2}{\Gamma^2} + 1\right)^4} \\ & + \frac{24G_0 \left(\frac{eV}{2} - E_{level}\right)}{e\Gamma^4 \left(\frac{4\left(\frac{eV}{2} - E_{level}\right)^2}{\Gamma^2} + 1\right)^3} + \frac{24G_0 \left(\frac{eV}{2} + E_{level}\right)}{e\Gamma^4 \left(\frac{4\left(\frac{eV}{2} + E_{level}\right)^2}{\Gamma^2} + 1\right)^3} \end{aligned} \quad (9)$$

$$\begin{aligned} \frac{d^5I}{dV^5} = & \frac{3072G_0 \left(\frac{eV}{2} - E_{level}\right)^4}{e\Gamma^8 \left(\frac{4\left(\frac{eV}{2} - E_{level}\right)^2}{\Gamma^2} + 1\right)^5} + \frac{3072G_0 \left(\frac{eV}{2} + E_{level}\right)^4}{e\Gamma^8 \left(\frac{4\left(\frac{eV}{2} + E_{level}\right)^2}{\Gamma^2} + 1\right)^5} \\ & - \frac{576G_0 \left(\frac{eV}{2} - E_{level}\right)^2}{e\Gamma^6 \left(\frac{4\left(\frac{eV}{2} - E_{level}\right)^2}{\Gamma^2} + 1\right)^4} - \frac{576G_0 \left(\frac{eV}{2} + E_{level}\right)^2}{e\Gamma^6 \left(\frac{4\left(\frac{eV}{2} + E_{level}\right)^2}{\Gamma^2} + 1\right)^4} \\ & + \frac{12G_0}{e\Gamma^4 \left(\frac{4\left(\frac{eV}{2} - E_{level}\right)^2}{\Gamma^2} + 1\right)^3} + \frac{12G_0}{e\Gamma^4 \left(\frac{4\left(\frac{eV}{2} + E_{level}\right)^2}{\Gamma^2} + 1\right)^3} \end{aligned} \quad (10)$$

$$\begin{aligned}
\frac{d^6 I}{dV^6} = & -\frac{61440G_0 \left(\frac{eV}{2} - E_{level}\right)^5}{e\Gamma^{10} \left(\frac{4\left(\frac{eV}{2} - E_{level}\right)^2}{\Gamma^2} + 1\right)^6} - \frac{61440G_0 \left(\frac{eV}{2} + E_{level}\right)^5}{e\Gamma^{10} \left(\frac{4\left(\frac{eV}{2} + E_{level}\right)^2}{\Gamma^2} + 1\right)^6} \\
& + \frac{15360G_0 \left(\frac{eV}{2} - E_{level}\right)^3}{e\Gamma^8 \left(\frac{4\left(\frac{eV}{2} - E_{level}\right)^2}{\Gamma^2} + 1\right)^5} + \frac{15360G_0 \left(\frac{eV}{2} + E_{level}\right)^3}{e\Gamma^8 \left(\frac{4\left(\frac{eV}{2} + E_{level}\right)^2}{\Gamma^2} + 1\right)^5} \\
& - \frac{720G_0 \left(\frac{eV}{2} - E_{level}\right)}{e\Gamma^6 \left(\frac{4\left(\frac{eV}{2} - E_{level}\right)^2}{\Gamma^2} + 1\right)^4} - \frac{720G_0 \left(\frac{eV}{2} + E_{level}\right)}{e\Gamma^6 \left(\frac{4\left(\frac{eV}{2} + E_{level}\right)^2}{\Gamma^2} + 1\right)^4}
\end{aligned} \tag{11}$$

## 4 Finite Temperature Effects

In deriving the model equations, we neglected finite temperature effects since the voltages used in the experiments are much larger than the average thermal energy at room temperature. The current at 1 V bias voltage differs less than 1% for the investigated systems when finite temperature effects are included. Specifically, if we consider a junction with a Lorentzian transmission with  $E_{level} = 1.1$  eV and  $\Gamma = 0.04$  eV (as determined for molecule **1**), we get a current of 32.56 nA at 300 K compared to a current of 32.27 nA at 0 K.

## 5 The Impact of Bias Voltage on Level Alignment and Coupling in Au Junctions

To investigate the effect of bias voltage on transmission characteristics, we determine  $E_{level}$  and  $\Gamma$  at 0.5 V, 0.75 V and 1.0 V DC for **1** and **2** with Au electrodes. In SI Figure S3, we observe that for both systems,  $\Gamma$ 's are almost identical at all three voltages. This shows that: (a) the molecule is not strongly polarized as this would induce changes in  $\Gamma$ ; (b) molecular vibrations are not activated as this would lead to an increased  $dG/dV$  resulting in a change in  $\Gamma$  and (c) local heating, if at all present, does not alter the results. We also note that there is a slight shift ( $\sim 0.1$  V) in  $E_{level}$  with increasing bias voltage away from the Fermi level. This could stem from a capacitive coupling, i.e. due to the molecule getting charged as the bias is increased, resulting in a small shift of the resonance; a second order Stark effect or small deviations from single Lorentzian transmission. Regardless of the underlying reason, this shows that the high bias measurements probe the zero bias transmission characteristics with a slight overestimation in  $E_{level}$ . Furthermore, these measurements provide experimental justification for single Lorentzian approximation as probing the transmission at different voltages yield almost identical results. We note that the experimental reason for doing all measurements at 1 V is that the nonlinearities in conductance with respect to voltage in Ag

junctions are too small to measure at lower DC bias voltages in **1**; while in molecule **2**, even at 1 V, we cannot carry out these measurements.

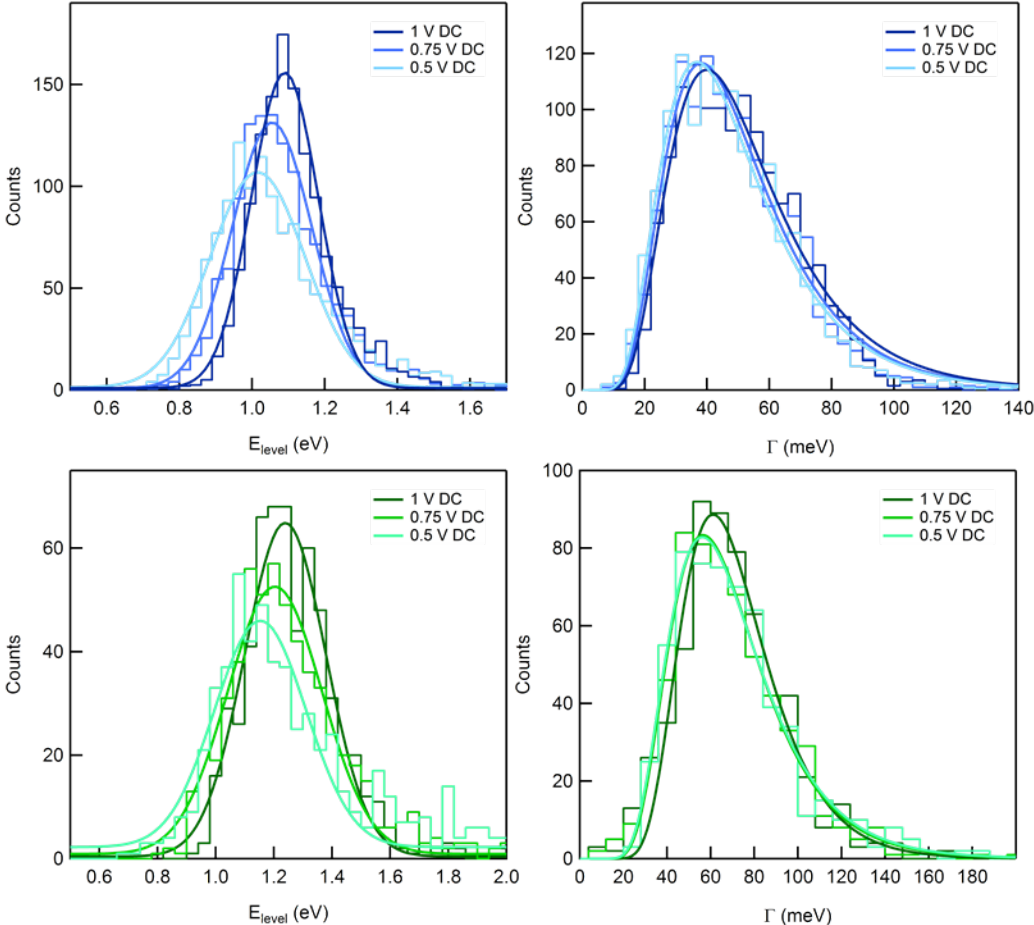


Figure S3. Histograms of  $E_{level}$  and  $\Gamma$  for molecule **1** (top) and molecule **2** (bottom) with Au electrodes measured at different bias voltages.

## 6 The Comparison Between Experimental and Simulated IV's

To benchmark the experimental technique, we measure IV curves and also carry out the AC technique for the same set of junctions with **1** and **2** using Au electrodes. This is done by holding a molecular junction, first measuring an IV curve and then applying an AC and DC voltage to determine  $E_{level}$  and  $\Gamma$  for each junction. We use the measured  $E_{level}$  and  $\Gamma$  to generate simulated IV curves using Equation 5 above for each junction. In SI Figure S4, we compare the measured and simulated two-dimensional IV histograms. An averaged measured IV curve is overlaid on both measured and simulated 2D-IV histograms. We see an

excellent agreement between the measured and simulated IV's in each system, demonstrating the strength of the new experimental technique we use here.

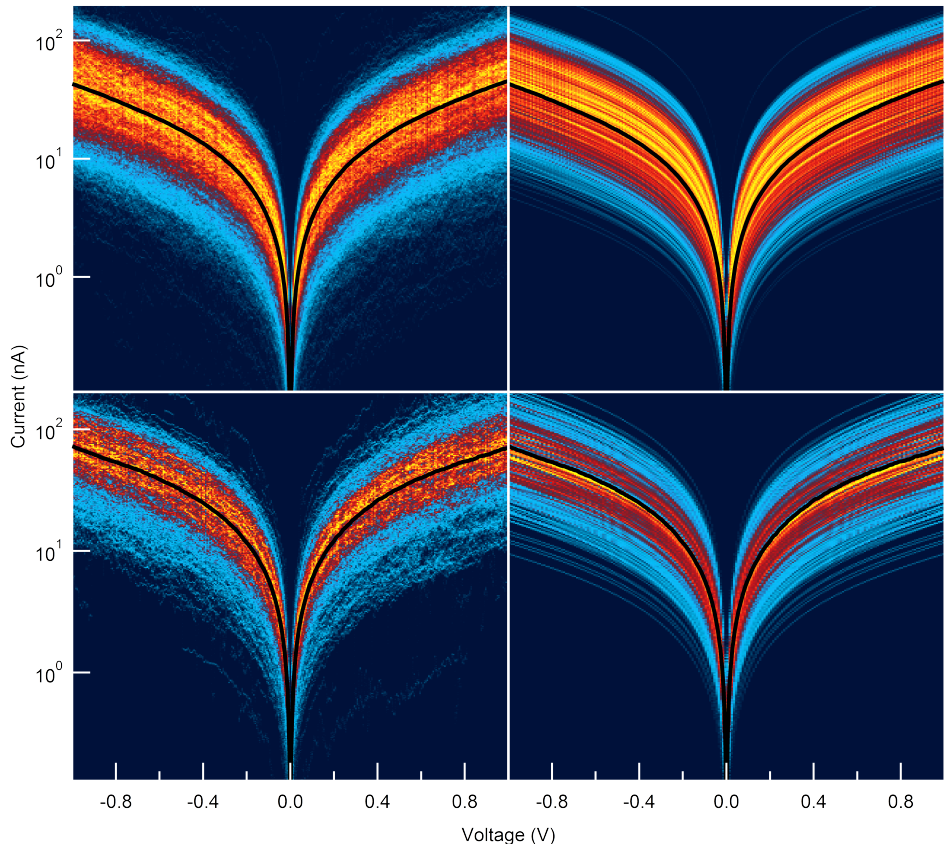


Figure S4. Experimental (left) and simulated (right) IV histograms for molecule **1** (top) and molecule **2** (bottom) with Au electrodes. Fits to the experimental IV's are overlaid onto the IV histograms for each molecule.

## 7 The Impact of Asymmetric Coupling on the Experimental Technique

The experimental technique relies on the assumption that the couplings of a single molecule junction are identical. Although the studied molecules have symmetric structures, they might still exhibit asymmetric couplings due to difference in binding geometries. Therefore, we need to examine the effect of asymmetric coupling on the experimental technique. For this purpose, we measured IV curves for **1** and **2** with Au electrodes. As shown in SI Figure S4, the IV histograms are very symmetric. However, if we look at individual IV's we see junctions exhibiting some asymmetry which gets averaged out in an IV histogram because the orientation of the molecule relative to the bias polarity is not controlled in our

experiments. To overcome this issue, we obtain IV histograms by flipping the polarity of individual IV curves that show higher current at positive voltage. We see that IV histograms obtained by flipping procedure exhibit 30% more current at -1 V compared to 1 V (see SI Figure S5). This implies that the molecular orbital moves with the applied voltage, i.e. the bias voltage drops asymmetrically, resulting in rectification. One way to have asymmetric voltage drop is to have asymmetric couplings however, we point out that voltage induced time dependent changes in the junction structure would also lead to asymmetric IV curves. In order to have 30% asymmetry in IV, a 6-8% asymmetry in the voltage drop is necessary for the molecular systems under study with single Lorentzian transmission with parameters reported in this work. If the entire asymmetry in voltage drop is due to asymmetry in coupling, couplings must differ by 30% according to Zotti, et.al.<sup>2</sup> The implications of these are two-fold: (a) the assumption of a transmission function with single coupling parameter does not hold and (b) the voltage drop is not symmetric. We examine the impact of these two findings separately.

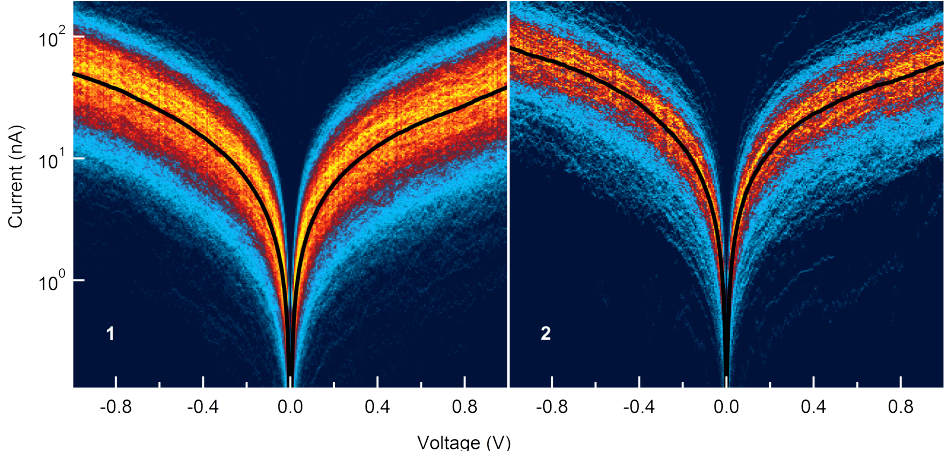


Figure S5. IV histograms for molecule **1** (left) and molecule **2** (right) with Au electrodes. Histograms are obtained by flipping the IV curves that show high current at positive polarity compared to negative polarity.

(a) The single-Lorentzian transmission with different couplings is modified to read:

$$T(E) = \frac{\Gamma_L \Gamma_R}{(E - E_{level})^2 + (\Gamma_L + \Gamma_R)^2/4} \quad (12)$$

where  $\Gamma = \Gamma_L + \Gamma_R$  following the standard convention. In our system,  $E - E_{level}$  is significantly larger than  $(\Gamma_L + \Gamma_R)/2$  and thus at all biases used in our measurements, we have:

$$T(E) = \frac{\Gamma_L \Gamma_R}{(E - E_{level})^2} \quad (13)$$

With this approximate transmission, in the presence of symmetric voltage drop, the experimental method measures twice the geometric mean of  $\Gamma_L$  and  $\Gamma_R$  instead of sum of two which leads to minor errors in the measured  $E_{level}$  and  $\Gamma$ .

(b) To investigate the impact of symmetric voltage drop on the experimental method, we perform Monte Carlo simulations. We sample pairs of  $E_{level}$  and  $\Gamma$  from Gaussian distributions with mean values and distribution widths similar to the experimentally observed ones. We generate, for each  $E_{level}$  and  $\Gamma$  pair, two pairs of  $G$  and  $dG/dV$  using single Lorentzian transmission and assuming voltage drop with an asymmetry of +8% and -8% to account for two possible orientations of the molecule relative to the bias. Next, we apply our analysis method used for the experiments to determine estimated  $E_{level}$  and  $\Gamma$  pairs for each true  $E_{level}$  and  $\Gamma$  pair using the generated  $G$  and  $dG/dV$  values. Note that our analysis method explicitly assumes that the voltage drop is symmetric. The results from the simulation are presented in SI Figure S6, where the estimated (red) and true (black) distributions of  $E_{level}$  and  $\Gamma$  are shown. We find that there is very little difference between the true distribution of  $\Gamma$  and the one obtained by assuming symmetric voltage drop in the presence of 8% asymmetry. This indicates that asymmetry in the voltage drop required to get 30% rectification does not lead to significant error in  $\Gamma$ . The estimated distribution of  $E_{level}$  is however distinguishably different from the true one. Specifically, we find that estimated distribution is bimodal, while the true distribution is Gaussian. However, since this is not what we see in the experiment (see Figure 3), we conclude that the actual asymmetry in voltage drop must be quite smaller than the one estimated from the asymmetric IV histograms. The observed asymmetry in the IV histograms is thus likely exaggerated by time-dependent changes in junction structure.

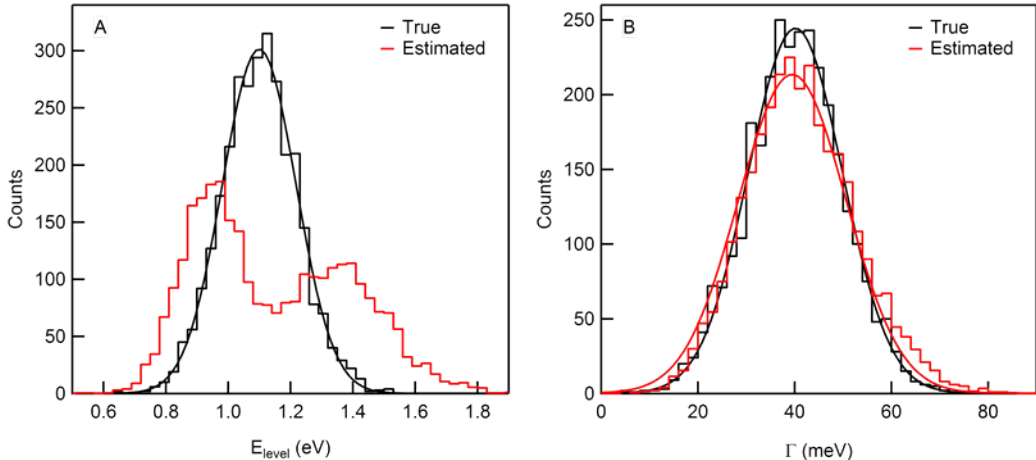


Figure S6. Monte Carlo simulations: True and estimated distributions of  $E_{level}$  (A) and  $\Gamma$  (B) when the voltage drop is asymmetric by 8% but is assumed to be symmetric.

## 8 Relativistic and non-Relativistic DFT Calculations

The DFT calculations are done using scalar relativistic corrections to the kinetic energy by pursuing the scaled zeroth order regular approximation.<sup>3</sup> Details of this implementation can be found in the work of Blum, et.al.<sup>4</sup>

As shown in SI Figure S7, we find that without relativistic corrections,  $\Gamma$  is similar for both Ag and Au junctions for molecule **1**. Specifically, we find that  $\Gamma_{Ag} = 38$  meV and  $\Gamma_{Au} = 52$  meV. With relativistic corrections,  $\Gamma_{Ag}$  increases by  $\sim 10\%$  to 42 meV while  $\Gamma_{Au}$  increases by  $\sim 50\%$  to 78 meV. As argued in the main text, this effect is related to the higher admixture of d-states of gold close to the Fermi level.

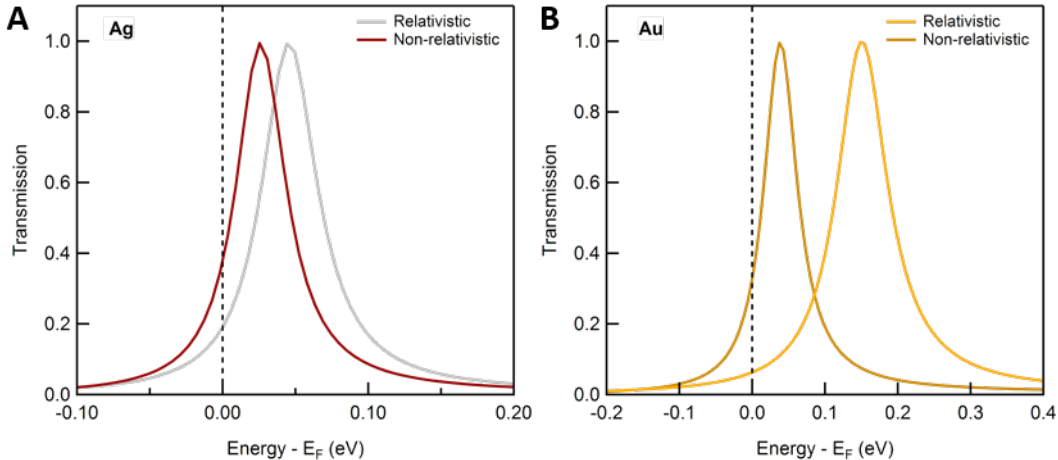


Figure S7. Calculated DFT based transmission curves with and without relativistic corrections for molecular junctions of **1** formed with (A) Ag and (B) Au electrodes.

## 9 References

1. Kim, T.; Vázquez, H.; Hybertsen, M. S.; Venkataraman, L. Nano Lett., 2013, 13, (7), 3358-3364.
2. Zotti, L. A.; Kirchner, T.; Cuevas, J. C.; Pauly, F.; Huhn, T.; Scheer, E.; Erbe, A. Small 2010, 6, 15291535
3. Lenthe, E. v.; Baerends, E. J.; Snijders, J. G. J. Chem. Phys., 1993, 99, (6), 4597-4610.
4. Blum, V.; Gehrke, R.; Hanke, F.; Havu, P.; Havu, V.; Ren, X.; Reuter, K.; Scheffler, M. Comp. Phys. Commun., 2009, 180, (11), 2175-2196.